Inorg. Chem. **2002**, *41*, 5787–5794

Reactivity of M^{II} Metal-Substituted Derivatives of Pig Purple Acid Phosphatase (Uteroferrin) with Phosphate

Mark B. Twitchett,[†] Gerhard Schenk,[†,‡] Manuel A. S. Aquino,[†] Douglas T.-Y. Yiu,[§] Tai-Chu Lau,[§] and A. Geoffrey Sykes*,[†]

Department of Chemistry, University of Newcastle, Newcastle upon Tyne NE1 7RU, U.K., Department of Biochemistry, University of Queensland, Brisbane 4072, Australia, and Department of Biology & Chemistry, City University of Hong Kong, Tat Chee Avenue, Hong Kong

Received January 14, 2002

The Fe^{II} of the binuclear $Fe^{II}Fe^{III}$ active site of pig purple acid phosphatase (uteroferrin) has been replaced in turn by five M^{II} ions (Mn^{II}, Co^{II}, Ni^{II}, Cu^{II}, and Zn^{II}). An uptake of 1 equiv of M^{II} is observed in all cases except that of Cu^{II}, when a second more loosely bound Cu^{II} is removed by treatment with edta. The products have been characterized by different analytical procedures and by UV–vis spectrophotometry. At 25 °C, $I = 0.100$ M (NaCl), the nonenzymatic reactions with $H_2PO_4^-$ give the μ-phosphato product, and formation constants K/M^{-1} show an 8-fold spread at pH 4.9 of 740 (Mn), 165 (Fe), 190 (Co), 90 (Ni), 800 (Cu), 380 (Zn). The variations in K correlate well with stability constants for the complexing of $H_2PO_4^-$ and $(CH_3O)HPO_3^-$ with M^{II} hexaaqua ions. At pH 4.9 with $[H_2PO_4^-] \geq 3.5$ mM rate constants k_{obs} decrease, and an inhibition process in which a second $[H_2PO_4^-]$ coordinates to the dinuclear center is proposed. The mechanism considered accounts for most but not all of the features displayed. Thus K_1 values for the coordination of phosphate to M^{II} are in the range10–60 M^{-1}, whereas K_2 values for the bridging of the phosphate to Fe^{III} are in the narrower range 7.8–12.4. From the fits described $K_i \sim 10^3$ M^{-1} for the inhibition step, which is independent of the identity of M^{II}. Values of k_{obs} decrease with increasing pH, giving pK_a values which are close to 3.8 and independent of M^{II} (Fe^{II}, Zn^{II}, Mn^{II}). The acid dissociation process is assigned to Fe^{III}–OH_2 to Fe^{III}–OH^-, where OH^- is less readily displaced by phosphate.

Introduction

Purple acid phosphatases (PAPs) are non-heme iron containing enzymes which have been isolated from mammals, plants, and fungal sources.[1−4] One of the most widely studied is uteroferrin (Uf) isolated from pig uteri ($M_r = 35$ kDa; 318 amino acids).[5] The active form of the enzyme has a binuclear $Fe^{II}Fe^{III}$ center, which catalyzes the hydrolysis of phosphate esters (eq 1).[1−4] Plant PAPs have also been

$$(RO)PO_3^{2-} + H_2O \rightarrow HPO_4^{2-} + ROH \qquad (1)$$

studied, e.g., kidney bean (kbPAP), which has a binuclear $Zn^{II}Fe^{III}$ center,[4,6,7] and in recent papers the $Mn^{II}Fe^{III}$ (sweet potato[8]) and $Zn^{II}Fe^{III}$ (sweet potato and soybean[8,9]) active sites have been reported. Different chemically substituted $M^{II}Fe^{III}$ sites have been reported with $M^{II} = Co^{II}$, Cu^{II}, Cd^{II}, Hg^{II}.[10−12]

X-ray crystal structures of the 111 kDa homodimeric (disulfide-bridged) $Zn^{II}Fe^{III}$ kbPAP enzyme (resolution 2.65 Å), the same protein with μ-phosphate coordinated (2.7 Å), and the product with μ-tungstate(VI) inhibitor coordinated (3.0 Å) have been reported.[7] More recently the structures of

* Author to whom correspondence should be addressed. E-mail: a.g.sykes@newcastle.ac.uk.
[†] University of Newcastle.
[‡] University of Queensland.
[§] City University of Hong Kong.

(1) Twitchett, M. B.; Sykes, A. G. *Eur. J. Inorg. Chem.* **1999**, 2105−2115.
(2) Sträter, N.; Lipscomb, W. N.; Klabunde, T.; Krebs, B. *Angew. Chem., Int. Ed. Engl.* **1996**, *35*, 2024−2055.
(3) Klabunde, T.; Krebs, B. *Struct. Bonding* **1997**, *89*, 177−198. (b) Schenk, G.; Guddat, L. W.; Ge, Y.; Carrington, L. E.; Hume, D. A.; Hamilton, S.; de Jersey, J. *Gene* **2000**, *250*, 117. (c) Schenk, G.; Korsinczky, M. L. J.; Hume, D. A.; Hamilton, S.; de Jersey, J. *Gene* **2000**, *255*, 419.
(4) Sträter, N.; Klabunde, T.; Tucker, P.; Witzel, H.; Krebs, B. *Science* **1995**, 1489.
(5) Chen, T. T.; Bazer, F. W.; Cetorelli, J. J.; Pollard, W. E.; Roberts, R. M. *J. Biol. Chem.* **1973**, *248*, 8560. (b) Baumbach, G. A.; Ketcham, C. M.; Richardson, D. A.; Bazer, F. W.; Roberts, R. M. *J. Biol. Chem.* **1986**, *261*, 12869.
(6) Beck, J. L.; de Jersey, J.; Zerner, B.; Hendrich, M. P.; Debrunner, P. *J. Am. Chem. Soc.* **1988**, *110*, 3317.
(7) Klabunde, T.; Sträter, N.; Fröhlich, R.; Witzel, H.; Krebs, B. *J. Mol. Biol.* **1996**, *259*, 737.
(8) Schenk, G.; Ge, Y.; Carrington, L. E.; Wynne, C. J.; Searle, I. R.; Carroll, B. J.; Hamilton, S.; de Jersey, J. *Arch. Biochiem. Biophys.* **1999**, *370*, 183. (b) Schenk, G.; Boutchard, C. L.; Carrington, L. E.; Noble, C. J.; Moubaraki, B.; Murray, K. S.; de Jersey, J.; Hanson, G. R.; Hamilton, S. *J. Biol. Chem.* **2001**, *276*, 19084.
(9) Durmus, A.; Eicken, C.; Sift, B. H.; Kratel, A.; Kappl, R.; Hüttermann, J.; Krebs, B. *Eur. J. Biochem.* **1999**, *260*, 709.

10.1021/ic020037f CCC: $22.00
Published on Web 10/10/2002

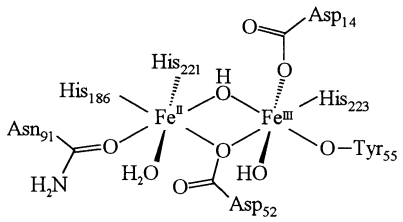

Figure 1. Structure of $Fe^{II}Fe^{III}$ active site of pig (uteroferrin) purple acid phosphatase.

μ-phosphato derivatives of mammalian PAPs (38 kDa) from Uf (1.55 Å)[13] and rat (2.7 Å),[14] in the $Fe^{III}Fe^{III}$ nonactive state, have been determined. The high-resolution Uf structure, Figure 1,[13] confirms octahedral coordination at both metals. From sequence homologies and spectroscopic studies there are similarities with kbPAP, and the dimetallic ligation appears to be identical for PAPs from different sources. Thus the two metals are bridged by a μ-hydroxo group and a single O atom of aspartate, and the α-carbon atoms of the seven coordinated amino acids superimpose. The bridging hydroxide and other structural features are supported by physical measurements.[15−17]

In addition three histidines (His-202, -295, and -296) are located near to the dimetallic center of kbPAP and are in positions where they can interact with free phosphate.[7] The corresponding residues in the mammalian PAPs are His-92, Glu-194, and His-195. In the mammalian structures it has been observed that His-92 and His-195 hydrogen bond to the bridging phosphate,[13,14] but no similar role is envisaged for Glu-194. The conservation of two of the histidines, Figure 2, and ability to superimpose the different structures suggest a mechanistic relevance.

In previous work on $Fe^{II}Fe^{III}$ Uf,[18] the reactions of different phosphates (referred to collectively as PO_4) have been studied, and the mechanism depicted in eqs 2 and 3 has been proposed. The reaction with $H_2PO_4^-$ can be regarded as a

$$\begin{array}{l} Fe^{II}\text{---}Fe^{III} + PO_4 \rightleftharpoons Fe^{II}\text{---}Fe^{III} + H_2O \\ \quad | \quad | \qquad\qquad\quad | \quad | \\ H_2O \;\; H_2O \qquad\quad PO_4 \;\; H_2O \end{array} \tag{2}$$

$$\begin{array}{l} Fe^{II}\text{---}Fe^{III} \rightleftharpoons Fe^{II}\text{---}Fe^{III} + H_2O \\ \quad | \quad | \qquad\quad \backslash \quad / \\ PO_4 \;\; H_2O \qquad\quad PO_4 \end{array} \tag{3}$$

prototype for ester hydrolysis of $(RO)PO_3^{2-}$. The pH dependence of reaction 3 has been assigned to acid dissociation of $Fe^{III}-OH_2$. To bring about ester hydrolysis the substitution

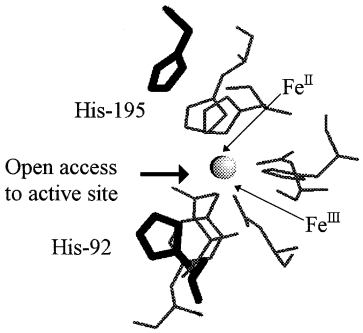

Figure 2. Structure of $Fe^{II}Fe^{III}$ active site of pig (uteroferrin) purple acid phosphatase showing access to the active site and the proximity of His-92 and His-195.

of the OH^- of $Fe^{III}-OH$ into the P^vcoordination sphere with displacement of RO^- has been proposed (eq 4).[18−20] Additional features have come to light in the present work.

$$\begin{array}{l} Fe^{II}\text{---}Fe^{III} \\ \quad | \quad | \\ ROPO_3 \;\; OH \end{array} \rightarrow \begin{array}{l} Fe^{II}\text{---}Fe^{III} \\ \quad \backslash \quad / \\ \quad HPO_4 \end{array} + RO^- \tag{4}$$

An appraisal of the effect of different M^{II} metals is of particular interest in view of the involvement of Fe^{II}, Zn^{II}, and Mn^{II} in naturally occurring PAP forms. In previous work the Zn^{II} for Fe^{II} substituted active site of pig PAP has been found to behave similarly to the $Zn^{II}Fe^{III}$ site of kbPAP,[6] and similarly Fe^{II} for Zn^{II} substituted kbPAP gives a catalytically active $Fe^{II}Fe^{III}$ form.[20]

Experimental Section

Isolation of PAP (Uteroferrin). Uteroferrin was obtained from the allantoic fluid of a sow at mid-pregnancy and purified according to literature procedures.[5,18] The purified $Fe^{III}Fe^{III}$ protein was reduced to the $Fe^{II}Fe^{III}$ state by addition of ascorbate (0.10 M) and dialyzed for 4 h against ammonium iron(II) sulfate (6 mM) at pH 5.0 (50 mM sodium acetate). This was followed by desalting on a Sephadex G25 column, and the buffer was exchanged using an Amicon filter with a PM10 membrane. The UV−vis absorbance (*A*) ratio for $Fe^{II}Fe^{III}$ Uf at different wavelengths A_{280}/A_{515} gave a value of less than 15:1 as required.[18] The protein was dialyzed against 40 mM acetate buffer at pH 4.9 and concentrated by Amicon filtration. Any remaining phosphate was removed from $Fe^{II}Fe^{III}$ Uf solutions by further desalting, and the final UV−vis spectrum corresponded to that of $Fe^{II}Fe^{III}$ Uf. The concentrated protein solution was separated into 1 mL aliquots and stored frozen at −80 °C under air.

Other Reagents. The following reagents were used as supplied: potassium dihydrogen (ortho)phosphate, KH_2PO_4 (Sigma); sodium dithionite (also referred to as hydrosulfite), $Na_2S_2O_4$

(10) Beck, J. L.; Keough, D. T.; de Jersey, J.; Zerner, B. *Biochim. Biophys. Acta* **1984**, *791*, 357.
(11) Beck, J. L.; McArthur, M. J.; de Jersey, J.; Zerner, B. *Inorg. Chim. Acta* **1988**, *153*, 39.
(12) Holz, R. C.; Que, L., Jr. *J. Am. Chem. Soc.* **1992**, *114*, 4434.
(13) Guddat, L. W.; McAlpine, A. S.; Hume, D.; Hamilton, S.; de Jersey, J.; Martin, J. L. *Structure* **1999**, *7*, 757.
(14) Uppenberg, J.; Lindquist, F.; Svensson, C.; Ek-Rylander, B.; Andersson, G. *J. Mol. Biol*. **1999**, *290*, 201. (b) Lindquist, Y.; Johansson, E.; Kaija, H.; Vikho, P.; Schneider, G. *J. Mol. Biol*. **1999**, *291*, 135.
(15) Gehring, S.; Fleischhauer, P.; Behlendorf, M.; Huber, M.; Lorösch, J.; Haase, W.; Dietrich, M.; Witzel, H.; Löcke, R.; Krebs, B. *Inorg. Chim. Acta* **1996**, *252*, 13.
(16) Averill, B. A.; Davis, J. C.; Burman, S.; Zirino, T.; Sanders-Loehr, J.; Moehr, T. M.; Sage, J. T.; Debrunner, P. G. *J. Am. Chem. Soc.* **1987**, *109*, 3760.
(17) Yang, Y.-S.; McCormick, J. M.; Solomon, E. I. *J. Am. Chem. Soc.* **1997**, *119*, 11832.
(18) Aquino, M. A. S.; Lim, J.-S.; Sykes, A. G. *J. Chem. Soc. Dalton Trans*. **1992**, 2135. (b) Aquino, M. A. S.; Lim, J.-S.; Sykes, A. G. *J. Chem. Soc., Dalton Trans*. **1994**, *429*.
(19) Merkx, M.; Pinkse, M. W. H.; Averill, B. A. *Biochemistry* **1999**, *38*, 9914.
(20) Suerbaum, H.; Körner, M.; Witzel, H.; Althaus, E.; Mosel, B.-D.; Müller-Warmuth, W. *Eur. J. Biochem*. **1993**, *214*, 313.

(Sigma); 2-mercaptoethanol, $HSCH_2CH_2OH$ (Aldrich); zinc(II) sulfate, $ZnSO_4 \cdot 7H_2O$ (Sigma); nickel chloride, $NiCl_2 \cdot 6H_2O$ (Aldrich); cobalt(II) chloride, $CoCl_2 \cdot 6H_2O$ (BDH); copper(II) sulfate, $CuSO_4 \cdot 5H_2O$ (Sigma); manganese(II) sulfate, $MnSO_4 \cdot H_2O$ (Sigma); bathophenanthroline disulfonic acid, 4,7-diphenyl-1,10-phenanthroline disulfonic acid, $Na_2C_{24}H_{14}N_2O_6S_2$, referred to here as DPS-phen (Sigma); 2,2′-biquinoline, $C_{18}H_{12}N_2$ (Sigma); sodium periodate, $NaIO_4$ (Analar, BDH). The disodium dihydrogen salt of edta (ethylenediaminetetraacetate) was used (Sigma). Stock solutions of phosphate were made up with the appropriate buffer (see below). Acid dissociation pK_a values for H_3PO_4 (2.12) and $H_2PO_4^-$ (6.7) indicate $H_2PO_4^-$ as the dominant reactant species for the range of pH values studied.[18] Monodentate and bridging phosphate products are assumed to be present as HPO_4^{2-} at pH 4.9; see, e.g., ref 21.

Buffers. Buffers (40 mM) used were as follows: glycine-HCl, pH 2.5−3.2; acetate-acetic acid, pH 3.2−5.6; and [bis(2-hydroxyethyl)amino]-[tris(hydroxymethyl)methane] (bis-tris)/(HCl), pH 5.6−6.2, all from Sigma. Previously the effect of acetate (which is potentially coordinating) was tested by variations in the range 25−55 mM, without any effect being observed.[18] Here runs were carried out with no acetate present using 4-chloroaniline (Lancaster Chemicals; pK_a 3.98) as buffer at pH 4.9. All buffer solutions were prepared using water that had been singly distilled, and then passed down a deionizer column.

Procedure for PAP Substitution. The procedure for the conversion of $Fe^{II}Fe^{III}$ enzyme to the apo-Fe^{III} containing product has been described.[10,11] This required the addition of a 10 μL aliquot of freshly prepared 1 M sodium dithionite to 1 mL of protein (60−300 μM) at pH 4.9 (100 mM acetate) to give $[S_2O_4^{2-}]$ (10 mM) under anaerobic conditions. After 1 min the mixture was separated using a small desalting column (150 × 5 mm, P6-DG desalting resin, BioRad). Within 2 min of elution metal-substituted PAP derivatives $Mn^{II}Fe^{III}$, $Co^{II}Fe^{III}$, $Ni^{II}Fe^{III}$, $Cu^{II}Fe^{III}$, and $Zn^{II}Fe^{III}$ respectively were generated by adding the M^{II} metal ion (50−650-fold excess) to the apo-Fe^{III} form (∼1 mL; 150−300 μM). β-Mercaptoethanol (0.12 M) was added in the case of Mn and Zn to facilitate metal uptake.[10] After ∼48 h the solution was again passed down a small desalting column and the metal-substituted derivative collected. Uptake of close to 2 equiv of Cu^{II} was observed, and treatment with edta was required to produce Uf that contained 1 equiv only of Cu^{II}.

Metal Analyses of $Fe^{II}Fe^{III}$ Uf PAP by ICP and Atomic Spectroscopy. Samples were prepared by digestion of a 1 mL sample with 1 mL of freshly prepared 1:1 solution of 30% hydrogen peroxide/concentrated nitric acid at 70 °C for 5 h until the solution became clear. The solution was cooled, diluted to 5 mL in a volumetric flask, and analyzed by an inductively coupled plasma (ICP) technique (using a Perkin-Elmer Plasma 1000) and by atomic absorption (Shimadzu AA-6502S). A sample of distilled water (1.0 mL) was digested in the same way and used as blank. Analysis for Fe gave exactly two per mole of PAP. Some Zn (∼7%) was detected, but Cu and Mn were below detection limits. Analyses for $Zn^{II}Fe^{III}$ Uf were also carried out.

PAP Metal Analyses by UV−Vis. The following additional procedures were used.

(a) Fe^{II}/Fe^{III} Content. The total Fe content was determined by reduction followed by complexation with DPS-phen.[22] The DPS-phen (0.4 mg) was dissolved in glacial acetic acid (400 μL) and then added to the protein (500 μL), which contained a small aliquot of L-cysteine to reduce the Fe^{III} to Fe^{II}. The total Fe was obtained by determining the absorbance of the $[Fe(DPS\text{-}phen)_3]^{2+}$ complex at 535 nm ($\epsilon = 2.21 \times 10^4$ M^{-1} cm^{-1}).

(b) Cu^{II} Content. The Cu^{II} of $Cu^{II}Fe^{III}$ Uf was determined by the Klotz method.[23,24] The reagent was prepared by adding 2,2′-biquinoline (50 mg) to glacial acetic acid (100 mL). To a sample of $Cu^{II}Fe^{III}$ Uf (500 μL) was added a small aliquot of L-cysteine in glacial acetic acid (100 μL) to reduce the Cu^{II} to Cu^{I}, followed by 2,2′-biquinoline solution (400 μL). The total Cu was determined as Cu^{I} by measuring the absorbance at 540 nm ($\epsilon = 6800$ M^{-1} cm^{-1}).

(c) Co^{II} Content. The Co^{II} of a solution of $Co^{II}Fe^{III}$ Uf (100 μL) was determined by addition of 11.3 M HCl (900 μL) to give 10.2 M HCl. After 2 min the blue color of tetrahedral Co^{II} species developed. Three major UV−vis peaks were observed at 624, 662, and 691 nm. From 10.2 M HCl solutions of known Co^{II} content, ϵ values of 350(10), 500(10), and 540(10) M^{-1} cm^{-1} respectively (errors in parentheses) were determined, and served to standardize the procedure.

(d) Mn^{II} Content. The Mn^{II} present in $Mn^{II}Fe^{III}$ Uf was determined by oxidation to permanganate with $NaIO_4$.[25] To the protein sample (1 mL) was added 18 M H_2SO_4 (100 μL), followed by $NaIO_4$ (10 mg), and the solution was heated for 10 min. After cooling, the purple colored permanganate solution was made up to 1.1 mL and the UV−vis spectrum recorded. Three peaks were observed at 507, 525, and 545 nm. From solutions of known Mn^{II} content, ϵ values of 1840(10), 2420(20), and 2300(20) M^{-1} cm^{-1} respectively were determined.

PAP Metal Analyses by Electrochemical Method. A Princeton Applied Research 173 potentiostat interfaced to an Elonex 486 IBM PC was used with EG & G software. Measurements were made at a gold disk electrode, which was polished prior to each experiment using an alumina powder (BDH, Analar, 0.3 μm diameter)/water slurry. The reference was an Ag/AgCl (1 M KCl) electrode in conjunction with a Pt-wire counter electrode.

(a) Cu^{II} Content. The Cu^{II} of $Cu^{II}Fe^{III}$ Uf was determined for aqueous protein solutions (1 mL) in glacial acetic acid (1 mL) by measurement of cyclic voltammogram peak heights. Scans were carried out over the range 700 to −300mV at a rate of 100 mV/s. The potential was held at −300 mV for 60 s to allow Cu metal to plate onto the electrode.

(b) Ni^{II} Content. The Ni^{II} component of $Ni^{II}Fe^{III}$ Uf was determined by the same procedure as for Cu^{II}. Scans were made over the range 0 to −500 mV at a rate of 100 mV/s. The potential was in this case held at −500 mV for 120 s.

Procedure for Determining Formation Constants for $H_2PO_4^-$ Binding to Uf. Overall formation constants K (25 °C) for the reaction of $H_2PO_4^-$ with $Fe^{II}Fe^{III}$ Uf were determined by UV−vis titrations at 680 nm (eq 5). Conditions were with protein (15−50

$$Fe^{II}Fe^{III} + H_2PO_4^- \overset{K}{\rightleftharpoons} Fe^{II}Fe^{III}\mu(HPO_4^{2-}) + H^+ \quad (5)$$

μM) at pH 4.9 (40 mM buffer), $I = 0.100$ M (NaCl). Absorbance changes were monitored on a Shimadzu 2101 PC spectrophotometer as small (microsyringe) aliquots of phosphate (200 mM) were added, final $[H_2PO_4^-]$ in the range 0.2−4.0 mM, $I = 0.100$ M

(21) Edwards, J. D.; Foong, S.-W.; Sykes, A. G. *J. Chem. Soc., Dalton Trans.* **1973**, 829.
(22) Zak, B. *Am. J. Clin. Pathol*. **1958**, *29*, 590.
(23) Klotz, I. M.; Klotz, T. A. *Science* **1955**, *121*, 477.
(24) Felsenfeld, G. *Arch. Biochem. Biophys*. **1960**, *87*, 247.
(25) Willard, H. H.; Greathouse, L. H. *J. Am. Chem. Soc*. **1917**, *39*, 2366.

Table 1. Metal Analyses for Different $M^{II}Fe^{III}$ Uf PAP Active Sites by Colorimetric or Electrochemical Methods (Error Range in Parentheses), Together with UV−Vis Peak Position (λ/nm) and Absorption Coefficients (ϵ/M^{-1} cm^{-1}) at pH 4.9 (40 mM Acetate), $I = 0.100$ (NaCl)

active site	Fe/mol	M^{II}/mol	λ	ϵ
$Fe^{II}Fe^{III}$	1.94(3)		510	4450
$Fe^{III}Fe^{III}$	1.91(4)		550	4300
apo-Fe^{III}	0.91(4)		545	3190
$Mn^{II}Fe^{III}$	0.93(3)	1.10(8)	514	3350
$Co^{II}Fe^{III}$	0.85(4)	0.81(5)	518	3370
$Ni^{II}Fe^{III}$	0.80(6)	0.81(6)[a]	510	3260
$Cu^{II}Fe^{III}$	0.79(5)	0.96(7)	545	3400
		1.05(9)[a]		
$Zn^{II}Fe^{III}$	0.76(4)	0.80(6)[b]	525	3580

[a] Electrochemical method. [b] See also ref 10.

(NaCl). The data were fitted to eq 6,

$$\frac{1}{(A_0 - A_{obs})} = \frac{K}{[H_2PO_4^-](A_0 - A_p)} + \frac{1}{(A_0 - A_p)} \qquad (6)$$

where A_0 and A_p are absorbance values for $Fe^{II}Fe^{III}$ and $Fe^{II}Fe^{III}\mu$-(HPO_4^{2-}), respectively, and A_{obs} is the experimental value at a particular [$H_2PO_4^-$]. A similar procedure was used for the determination of K for the reaction of $H_2PO_4^-$ with different $M^{II}Fe^{III}$ Uf derivatives.

Kinetic Procedures. The reactions of $Fe^{II}Fe^{III}$ Uf and $M^{II}Fe^{III}$ derivatives with $H_2PO_4^-$ were monitored at wavelengths ~680 nm using an Applied Photophysics SX-17MV stopped-flow spectrophotometer. Absorbance vs time changes gave satisfactory uniphasic first-order fits, and hence rate constants k_{obs} using Applied Photophysics software. Average k_{obs} values from five triggerings were recorded. Protein concentrations were generally ~45 μM, and [$H_2PO_4^-$] values in the range 3.8−50 mM. The temperature was 25.0 ± 0.1 °C, and the ionic strength adjusted to $I = 0.100 \pm 0.001$ M with NaCl. From studies on the reaction of α-naphthyl phosphate with $Fe^{II}Fe^{III}$ Uf in which the formation of α-naphthol at 323 nm was monitored, maximum activity is observed at pH 4.9.[18] This pH applies also to studies on $M^{II}Fe^{III}$ Uf. However because of the mechanism proposed, an extension of the simple enzyme kinetic treatment may not apply, and more detailed activity studies are not considered in this work. Linear and nonlinear data fitting was carried out using the software Mac Curve Fit, version 1.1.2 (Kevin Raner Software).

Results

Characterization of Metal-Substituted Uteroferrin Derivatives. The metal ion content and UV−vis peaks/absorption coefficients (based on Fe^{III} content) for $Fe^{II}Fe^{III}$, $Fe^{III}Fe^{III}$, apo-Fe^{III}, and metal-substituted $M^{II}Fe^{III}$ Uf derivatives are as listed in Table 1. All metal determinations were an average of at least three values, with standard deviations as indicated. The derivatives contain close to one Fe^{III} to one atom of M^{II} per molecule of enzyme. An exception was with the initial Cu^{II} product. Following a typical reconstitution procedure, two Cu^{II} atoms per enzyme were incorporated per iron. To remove one of the Cu^{II}'s, edta (100μM) was added to the protein solution, which was allowed to stand for ~30 s before being passed down a desalting column. The activity of the $Cu^{II}Fe^{III}$ Uf before and after edta treatment was similar (see later), indicating that the active-site copper is selectively retained. The second Cu^{II} binds less strongly

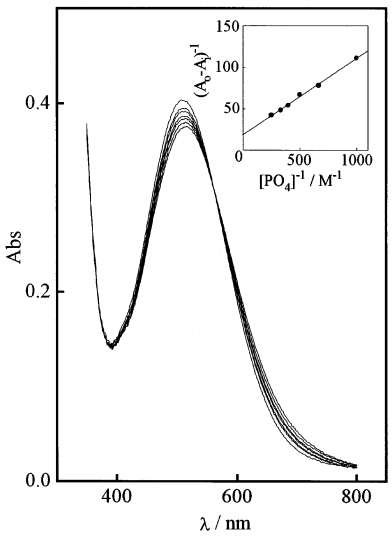

Figure 3. Determination of K (25 °C) by titration of 0.20 M $H_2PO_4^-$ (0−4 mM) with in this example $Co^{II}Fe^{III}$ Uf (~120 μM) at pH 4.90. The absorbance (A) at ~518 nm increases as $H_2PO_4^-$ is added, $I = 0.100$ M (NaCl). The inset plot of absorbance changes at 680 nm according to eq 6 allows K to be determined.

at an alternative site on the protein. The M^{II} products are different shades of purple consistent with retention of the dominant tyrosine phenolate to Fe^{III} ligand to metal charge-transfer (LMCT) transition.[26] The 500−550 nm peak absorption coefficients fall into two categories: those for the $Fe^{II}Fe^{III}$ and $Fe^{III}Fe^{III}$ protein, which are ~4400 M^{-1} cm^{-1}, and those for other $M^{II}Fe^{III}$ Uf forms, which are ~25% smaller.

Formation Constants K for $H_2PO_4^-$ Binding to $M^{II}Fe^{III}$ Uf. These, as defined in eq 5, were determined by UV−vis titration, absorbance changes as in Figure 3. Two stages, eqs 7 and 8, are proposed, with $K = K_1K_2$. No evidence was

$$\begin{array}{l} M^{II}\text{---}Fe^{III} \\ \quad | \quad | \\ H_2O \quad OH \end{array} + H_2PO_4^- \overset{K_1}{\rightleftharpoons} \begin{array}{l} M^{II}\text{---}Fe^{III} \\ \quad | \quad | \\ H_2PO_4 \quad OH \end{array} + H_2O \qquad (7)$$

$$\begin{array}{l} M^{II}\text{---}Fe^{III} \\ \quad | \quad | \\ H_2PO_4 \quad OH \end{array} \overset{K_2}{\rightleftharpoons} \begin{array}{l} M^{II}\text{---}Fe^{III} \\ \quad \backslash \quad / \\ \quad HPO_4 \end{array} + H_2O \qquad (8)$$

obtained for an [$H_2PO_4^-$]^2 dependence. Diphosphate $M^{II}Fe^{III}$ products are assumed to absorb less strongly than μ-phosphate products, with eq 5 defining the major part of absorbance changes observed. Values of K, Table 2, increase as the pH increases from 3.55 to 6.60. Acid dissociation of the $Fe^{III}-H_2O$ is proposed to account for this trend.

Variation of Rate Constants k_{obs} for $M^{II}Fe^{III}$ Uf with [$H_2PO_4^-$]. Values of k_{obs} in Table 1S (Supporting Information) include a set in which the acetate buffer was replaced by 4-chloroaniline. This replacement has no effect on k_{obs}, Figure 4, and it can be concluded that acetate does not coordinate appreciably.[18] At pH 4.9 first-order rate constants

(26) Doi, K.; McCracken, J.; Peisach, J.; Aisen, P. *J. Biol. Chem.* **1988**, *263*, 5757.

Table 2. Formation Constants K (25 °C) for $H_2PO_4^-$ Binding to $Fe^{II}Fe^{III}$ Uf and $M^{II}Fe^{III}$ Uf (15−50 μM), 40 mM Acetate Buffer, I = 0.100 M (NaCl) (Standard Deviations in Parentheses)

protein	pH	K/M^{-1}
$Fe^{II}Fe^{III}$	3.55	80(10)
	4.90	165(25)[a]
	6.60[b]	1140(160)
$Mn^{II}Fe^{III}$	4.90	740(50)
$Co^{II}Fe^{III}$	4.90	190(30)
$Ni^{II}Fe^{III}$	4.90	90(10)
$Cu^{II}Fe^{III}$	4.90	800(55)
$Zn^{II}Fe^{III}$	4.90	380(30)

[a] Previous values in range 83−313 M^{-1}. [b] Bis-tris buffer.

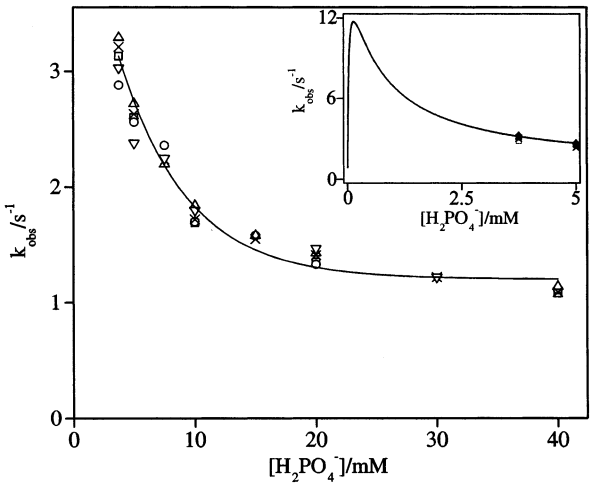

Figure 4. The variation of first-order rate constants k_{obs} (25 °C) with $[H_2PO_4^-]$ for the reaction of $Fe^{II}Fe^{III}$ Uf (10−40 μM) with $H_2PO_4^-$ at pH 4.9, I = 0.100 M (NaCl). Different data sets □ (air-free), ○, △ and × (in air), all using 45 mM acetate buffer, and ▽ with 18 mM 4-chloroaniline buffer (also in air), indicate satisfactory reproducibility. The solid line generated by fitting to eq 10 is shown, and in the inset this is extended to low $[H_2PO_4^-]$.

k_{obs} for the reaction of $H_2PO_4^-$ with $Fe^{II}Fe^{III}$ Uf monitored at 620 nm show little dependence on $[H_2PO_4^-]$ in the range 25−45 mM, as observed previously.[18] At $[H_2PO_4^-]$ < 20 mM, however, an upward trend in k_{obs} is apparent and is reproducible under different conditions. Similar behavior is observed for the M^{II} substituted derivatives, Table 2S (Supporting Information) and Figure 5. Errors for k_{obs} (Tables 1S and 2S) are ±9% at low pH and ±3% at higher pH. A satisfactory fit to the empirical eq 9 is obtained, Figure 6.

$$k_{obs} = A[H_2PO_4^-]^{-1} + B \qquad (9)$$

Since $k_{obs} = 0$ at $[H_2PO_4^-] = 0$, a dependence as in Figure 4 (inset) is indicated, and an inhibition step K_i is included in the reaction sequence (Scheme 1), from which eq 10 is obtained.

$$k_{obs} = k_f\{K_1[H_2PO_4^-]\}/\{1 + K_1[H_2PO_4^-] + K_1K_i[H_2PO_4^-]^2 + K_1K_2[H_2PO_4^-]\} + k_b \qquad (10)$$

At high $[H_2PO_4^-]$ this simplifies to the same form as eq 9 with A and B respectively k_f/K_i and k_b. An examination of the fit (inset to Figure 4) makes clear the extent to which data is extrapolated, and draws attention to uncertainties in the quality of the fit. Hence the algorithm for the fitting is very sensitive to estimates of the fitted parameters. The following approach was taken to gain reasonable estimates. Approximate values for k_b were obtained from the linear plots in Figure 6 and were used as initial estimates in eq 10. Satisfactory fits were obtained with $K_i \sim 10^3$ M. Finally, the number of variables was reduced by replacing K_2 by the ratio k_f/k_b. In the first round of fitting k_b and K_i were kept constant. This restriction was subsequently released to obtain an improved fit (fit 1). Last, K_2 was substituted back into eq 10 and the fit was rerun (fit 2 is shown in Figure 4). It turns out that K_i does not change significantly; furthermore the same fit was obtained when an initial value of K_i in the range 0.9−1.2 mM was chosen (data not shown). Likewise rate

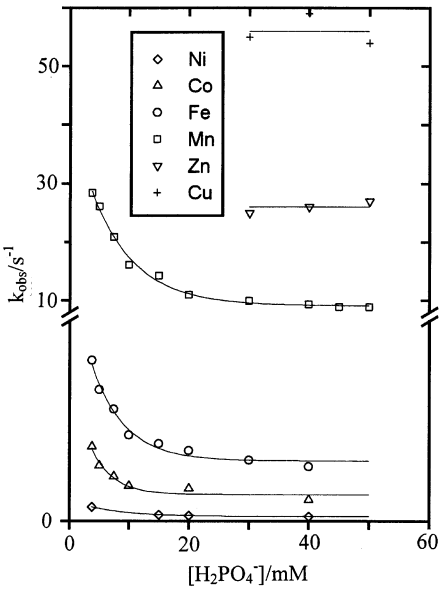

Figure 5. The variation of first-order rate constants k_{obs} (25 °C) for the reactions of $M^{II}Fe^{III}$ Uf (10−40 μM), M = Fe^{II}, Mn^{II}, Co^{II}, Ni^{II}, Cu^{II}, Zn^{II} with $[H_2PO_4^-]$ at pH 4.9, I = 0.100 M (NaCl).

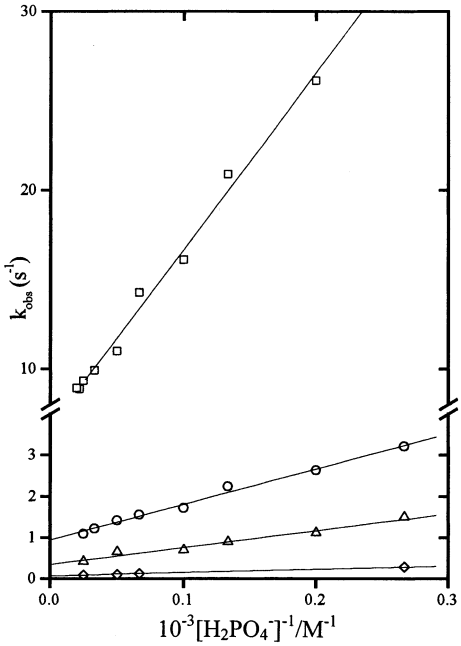

Figure 6. The variation of first-order rate constants k_{obs} (25 °C) with $[H_2PO_4^-]^{-1}$ for the reaction of $H_2PO_4^-$ with $Mn^{II}Fe^{III}$ Uf (□), $Fe^{II}Fe^{III}$ Uf (○), $Co^{II}Fe^{III}$ Uf (△), and $Ni^{II}Fe^{III}$ Uf (◇), at pH 4.9.

Scheme 1

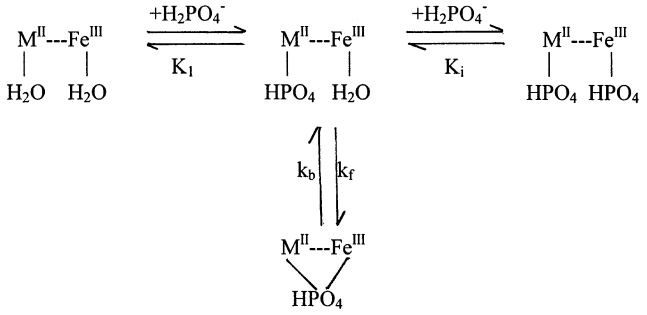

Table 3. Fit of Average Rate Constants k_{obs} at pH 4.9 to Eq 10 (Weighted According to Spread at Each $[H_2PO_4^-]$) Using a Fixed Value for K_i of $\sim 10^3$ M^{-1}; Other Terms as Defined in Scheme 1

derivative	k_f/s^{-1}	k_b/s^{-1}	K_1/M^{-1}	K_2
$Fe^{II}Fe^{III}$ [a]	6.9	0.91	27	7.8[b] (7.6[c])
$Mn^{II}Fe^{III}$	84.5	7.1	60	12.4[b] (11.9[c])
$Co^{II}Fe^{III}$	4.1	0.36	18	12.1[b] (11.4[c])
$Ni^{II}Fe^{III}$	0.91	0.094	10	9.7[b] (9.6[c])

[a] Five data sets used, Table 1S. [b] Fit 2 (see text). [c] From ratio k_f/k_b (Fit 1).

constants for the opening of the μ-phosphato bridge k_b in eq 10 are very similar (factor of 1.6), and are as listed in Table 3. Values of K_2 obtained from fit 1 and fit 2 are indicated, and a reasonable agreement is found.

Similar behavior is obtained at pH = 4.6, the pH used in earlier studies.[18] Values of k_{obs} for the $M^{II}Fe^{III}$ reaction vary by $\sim 10^3$ at high $[H_2PO_4^-]$, ranging from 0.062 s^{-1} for Ni^{II}-Fe^{III} Uf to 57 s^{-1} for $Cu^{II}Fe^{III}$ Uf. Variations for the different $M^{II}Fe^{III}$ Uf derivatives are attributed to the different M^{II} reactivities with $[H_2PO_4^-]$ (i.e., K_1). No UV−vis changes were observed on addition of $H_2PO_4^-$ to apo-Fe^{III} protein.

pH Dependence of Rate Constants k_{obs} for $M^{II}Fe^{III}$ Uf with $H_2PO_4^-$. Here the pH dependences of rate constants for $Fe^{II}Fe^{III}$ Uf, $Zn^{II}Fe^{III}$ Uf, and $Mn^{II}Fe^{III}$ Uf are considered. Stopped-flow first-order rate constants k_{obs} (Table 3S, Supporting Information) are dependent on pH in the range 3.0−6.2, Figure 7. A single pK_a effect is dominant, which is attributed to the deprotonation of the Fe^{III} bound water.[18]

Discussion

In these studies five $M^{II}Fe^{III}$ Uf substituted derivatives (M^{II} = Mn^{II}, Co^{II}, Ni^{II}, Cu^{II}, Zn^{II}) of pig $Fe^{II}Fe^{III}$ PAP (Uf) have been prepared and characterized. As part of the characterization, details of the UV−vis absorbance peaks (λ and ϵ values) have been obtained, Table 1. Derivatives incorporating Mn^{II} and Ni^{II} have been studied for the first time. The Mn^{II} and Zn^{II} products are of particular interest because plant PAP forms with $Zn^{II}Fe^{III}$ and $Mn^{II}Fe^{III}$ active sites are known.[7−9] Metal analyses indicate that all the derivatives have close to one Fe^{III} and one M^{II} per Uf molecule. An exception is with the Cu^{II} derivative, where the initial product binds two Cu^{II} atoms. The second Cu^{II} does not greatly perturb the Cu^{II}-Fe^{III} reactivity and is selectively removed by treatment with edta. The tendency for two Cu^{II} ions to become incorporated may be due to the increased affinity of Cu^{II} for surface N-donor groups.

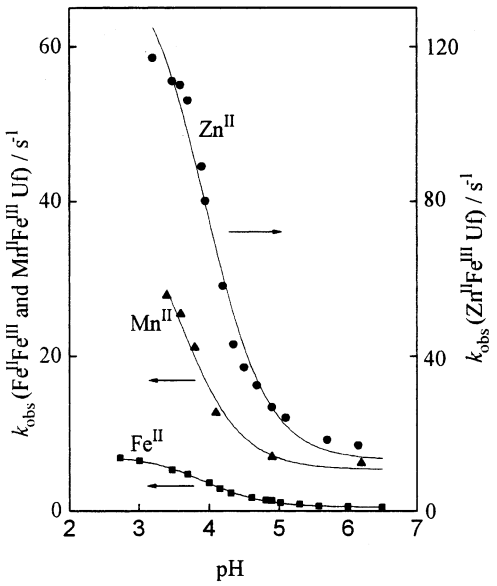

Figure 7. The variation of first-order rate constants k_{obs} (25 °C) with pH for the reaction of $H_2PO_4^-$ with native $Fe^{II}Fe^{III}$ Uf (■), $Mn^{II}Fe^{III}$ Uf (▲), and $Zn^{II}Fe^{III}$ Uf (●); protein concentrations (10−40 μM), $[H_2PO_4^-]$ (5−45 mM), pH = 2.7−6.5, I = 0.100 M (NaCl).

In the case of kbPAP three histidines His-202, His-295, and His-296 have been identified close to the active site, flanking entry to the $Zn^{II}Fe^{III}$.[7] Of these, His-202 and His-296 are conserved in the mammalian forms as His-92 and His-195, Figure 2. The X-ray structures of mammalian Fe^{III}-Fe^{III} forms have indicated H-bonding of these histidines to a bridging phosphate.[13,14] The histidines are also able to provide an initial point of contact of $H_2PO_4^-$ and other phosphate reagents with the PAP prior to binding to the dinuclear $M^{II}Fe^{III}$ site. Binding of the second Cu^{II} to the His-92 and His-195 residues adjacent to the active site seems unlikely, since in kinetic studies with $H_2PO_4^-$, rate constants for the product with a second Cu^{II} attached are similar to those with only a single Cu^{II} present.

The mechanism proposed previously for the reaction of $H_2PO_4^-$ with $Fe^{II}Fe^{III}$ Uf involves binding to the Fe^{II} in a relatively rapid process, which does not contribute appreciably to UV−vis absorbance changes, followed by bridging to the more strongly chromophoric Fe^{III}.[18] Such a reaction sequence is consistent with properties of high-spin Fe^{II} and Fe^{III} ions, the hexaaqua ions of which have water-exchange rate constants close to 10^6 s^{-1} and 10^3−10^4 s^{-1}, respectively.[27−29] The M^{II} hexaaqua ions are also more labile than the Fe^{III} ion. The reaction sequence eq 2−eq 3[18] has been modified to account for the more complex rate dependence on $[H_2PO_4^-]$, as illustrated in Figures 4 and 5. The experimental data were fitted to eq 10, which is derived for the reaction sequence in Scheme 1. Here, K_1, K_2, and K_i describe the equilibria for the binding of $H_2PO_4^-$, the formation of a μ-phosphato bridge, and the binding of a second $H_2PO_4^-$ to the active site, respectively, the latter

(27) Lincoln, S. F.; Merbach, A. E. *Adv. Inorg. Chem.*; Academic Press: New York, 1995; Vol. 42, pp 2−88.
(28) Swaddle, T. W.; Merbach, A. E. *Inorg. Chem.* **1981**, *20*, 4212.
(29) See, for example: Wilkins, R. G. In *Kinetics and Mechanism of Reactions of Transition Metal Complexes*; VCH: Weinheim, 1991.

giving the inhibition effect apparent in the inset to Figure 4.

Since K_2 describing the bridging process (Scheme 1) involves ligand substitution at the Fe^{III} site, it is not expected to depend greatly on the identity of the divalent metal ion. Consistent with this, values obtained for the different M^{II} identities lie within a factor of 1.6 (Table 3). Likewise K_i ($\sim 10^3$ M^{-1}) for the binding of free $H_2PO_4^-$ to Fe^{III} does not appear to vary appreciably with the identity of M^{II}. In contrast K_1 varies from 10 for Ni^{II} to 60 for Mn^{II}, supporting a mechanism in which there is binding of $H_2PO_4^-$ to the divalent metal ion.

As far as the formation constant K_1 is concerned, two stages, eqs 11 and 12 , seem likely. Prior association of

$$M^{II}\text{---}Fe^{III} + H_2PO_4^- \overset{K_{ass}}{\rightleftharpoons} M^{II}\text{---}Fe^{III}, H_2PO_4^- \quad (11)$$

$$M^{II}\text{---}Fe^{III}, H_2PO_4^- \overset{K_1'}{\rightleftharpoons} M^{II}\text{---}Fe^{III} + H_2O \quad (12)$$

$H_2PO_4^-$ with the two histidine residues His-92 and His-195 is consistent with the mechanism proposed by Sträter et al. for kbPAP.[4] The overall formation constant K_1 for $H_2PO_4^-$ binding at the M^{II} can therefore be modified to read $K_{ass}K_1'$. Studies on the oxidation of $Fe^{II}Fe^{III}$ Uf with $[Fe(CN)_6]^{3-}$ have provided evidence for a prior association.[30] Thus the saturation kinetics observed are consistent with eqs 13 and 14,

$$Fe^{II}Fe^{III} + [Fe(CN)_6]^{3-} \overset{K_{Fe}}{\rightleftharpoons} Fe^{II}Fe^{III}, [Fe(CN)_6]^{3-} \quad (13)$$

$$Fe^{II}Fe^{III}, [Fe(CN)_6]^{3-} \overset{k_{Fe}}{\rightarrow} Fe^{III}Fe^{III} + [Fe(CN)_6]^{4-} \quad (14)$$

where K_{Fe} is in this case K_{ass} for the association of $[Fe(CN)_6]^{3-}$, and k_{Fe} is for electron transfer from Fe^{II} to the $[Fe(CN)_6]^{3-}$. At 25 °C, pH 5.0, the kinetic treatment gives $K_{Fe} = 540$ M^{-1}, $I = 0.100$ M (NaCl). Competitive inhibition is observed with redox inactive $[Cr(CN)_6]^{3-}$ and $[Mo(CN)_8]^{4-}$, when association constants defined as in eq 13 give $K_{Cr} = 550$ M^{-1} and $K_{Mo} = 1580$ M^{-1}.[30] Smaller values of K_{ass} are expected in the case of the 1− reactant $H_2PO_4^-$.

Values of K (Table 2) for the formation step, eq 5, give an 8-fold spread for $M^{II} = Cu^{II} > Mn^{II} > Zn^{II} > Co^{II} \sim Fe^{II} > Ni^{II}$. These values (Figure 8a) are compared with those for 1:1 complexing of M^{II} hexaaqua ions with HPO_4^{2-} and $(CH_3O)PO_3^{2-}$ (Figure 8b).[31−33] The similar trends are of interest with the anomalous position of Cu^{II} as expected for the Irving−Williams series. Previous observations[33,34] that phosphate does not follow strictly the Irving−Williams sequence appear to be confirmed by the present studies.

Surprisingly both the rate constants k_f and k_b (Table 3) give $\sim 10^2$ variations as M^{II} is varied. In the case of k_b there

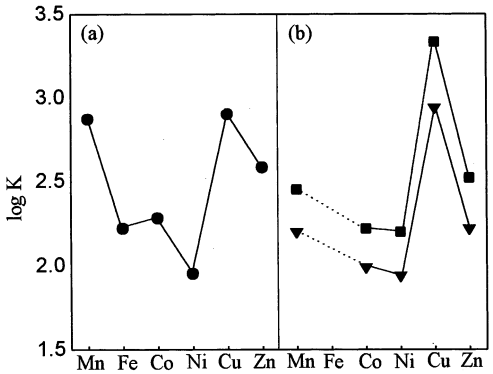

Figure 8. The variation of formation constants K (25 °C) with M^{II} atomic number: (a) for $M^{II}Fe^{III}$ Uf derivatives with $H_2PO_4^-$ (●) at pH 4.9; and (b) for the complexing of hexaaqua metal ions with HPO_4^{2-} (■) and $(MeO)PO_3^{2-}$ (▼).[31]

are two alternative mechanisms for the dissociation of the μ-PO_4 bridge, by cleavage of (i) $M^{II}-OPO_3$ or (ii) $Fe^{III}-OPO_3$. The spread observed suggests that alternative (i) applies, since for a common $Fe^{III}-OPO_3$ cleavage values would be expected to be similar and independent of M^{II}. In the case of k_f for HPO_4^{2-} bridging to Fe^{III} a $\sim 10^2$ spread of values is not expected, suggesting that the fitting procedure is not sufficiently precise or that the mechanism proposed requires some further modification.

The pH dependences of k_{obs} for $M^{II}Fe^{III}$ Uf ($M^{II} = Fe^{II}$, Zn^{II}, Mn^{II}) with $H_2PO_4^-$ are shown in Figure 7. The downward trend with increasing pH is assigned to acid dissociation of the more acidic $Fe^{III}-H_2O$, eq 15. Thus

$$Fe^{III}\text{-}OH_2 \overset{K_{1a}}{\rightleftharpoons} Fe^{III}\text{-}OH + H^+ \quad (15)$$

pK_{1a} is the main contribution to the trends observed, and from fits carried out values of 3.9, 3.9, and 3.6 respectively are obtained. Rate constants for bridge closure in eq 16

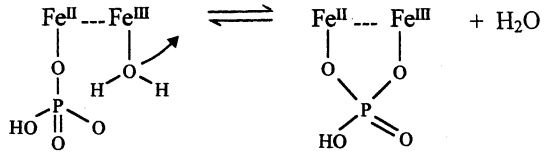

(16)

decrease at the higher pH's as $Fe^{III}-OH_2$ is replaced by $Fe^{III}-OH^-$, because anionic phosphate does not as readily displace OH^- as H_2O. In the case of the phosphate ester $ROPO_3^{2-}$, eq 17, the displacement of OR^- on the P^V by the OH^- results in ester hydrolysis. The activity of this process peaks at pH$\sim$4.9 when maximum $Fe^{III}-OH^-$ is present.

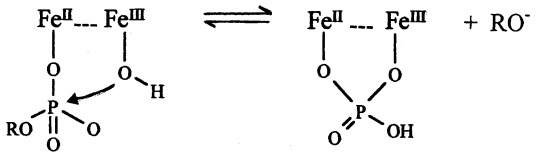

(17)

(30) Aquino, M. A. S.; Sykes, A. G. *J. Chem. Soc., Dalton Trans*. **1994**, *683*.
(31) Saha, A.; Saha, N.; Ji, L.-N.; Zhao, J.; Gregan, F.; Sajadi, S. A. A.; Song, B.; Sigel, H. *J. Biol. Inorg. Chem*. **1996**, *1*, 231.
(32) Sigel, H.; McCormick, D. B. *Acc. Chem. Res*. **1970**, *3*, 201−208.
(33) Sigel, H.; Song, B. *Met. Ions Biol. Syst*. **1996**, *32*, 135−205.
(34) Shriver, D. F.; Atkins, P. W. In *Inorganic Chemistry*, 3rd ed.; Oxford University Press: Oxford, 1990; p 244.

To summarize, in these studies the Fe^{II} of $Fe^{II}Fe^{III}$ Uf has been replaced in turn by Mn^{II}, Co^{II}, Ni^{II}, Cu^{II}, and Zn^{II} and the products characterized. The use of $H_2PO_4^-$ as a substrate helps define steps relevant to the ester hydrolysis of $ROPO_3^-$. Various parameters have been determined including K ($=K_1K_2$) for the formation of the μ-phosphate $M^{II}Fe^{III}$ Uf products. The dependence of rate constants k_{obs} for the equilibration of $M^{II}Fe^{III}$ Uf with $H_2PO_4^-$ is more complex than previously indicated, and is accounted for by inclusion of an inhibition step involving a second $H_2PO_4^-$ as shown in Scheme 1. From a fit to the rate law (eq 10), K_1 for substitution on M^{II} ($10-60\ M^{-1}$), K_2 ($=k_f/k_b$) for μ-phosphate formation (7.8−12.4), and $K_i \sim 10^3\ M^{-1}$ are obtained, which can be rationalized in terms of an involvement of M^{II} (variable) or Fe^{III} (invariable). Values of K_1 for the $H_2PO_4^-$ binding to M^{II} very likely incorporate K_{ass} for the prior association of $H_2PO_4^-$ to His-92 and His-195. Trends observed in k_f are less well understood. The pH dependence of rate constants k_{obs} indicates that the replacement of OH^- of $Fe^{III}-OH^-$ by M^{II}-attached HPO_4^{2-} to give the μ-phosphate product is not as rapid as when $Fe^{III}-OH_2$ is present. In these studies an order of effectiveness $Fe^{II} < Zn^{II} < Mn^{II}$ is observed for K, and $Fe^{II} < Mn^{II} < Zn^{II}$ for k_{obs}, with Fe^{II} showing the more controlled behavior.

Acknowledgment. We are grateful to the UK Engineering and Physical Sciences Research Council for financial support, and Wellcome Foundation for a Travel Grant (to G.S.). We thank Professor L. Que, Jr. (Minneapolis), for a sample of Zn^{II} Fe^{III} Uf at the commencement of this work, and Dr. B. Horrocks (Newcastle) for helpful discussion and access to electrochemical equipment. A.G.S. is grateful to City University, Hong Kong, for a position as Visiting Professor during 2001, and G.S. to the University of Queensland for leave of absence.

Supporting Information Available: Tables 1S, 2S, and 3S with listing of rate constants. This material is available free of charge via the Internet at http://pubs.acs.org.

IC020037F